11.2 Deuterium Permeation through Flibe Facing Materials

S. Fukada[a], R. A. Anderl[b], G. R. Smolik[b], R. J. Pawelko[b], S. T. Schuetz[b], J. P. Sharpe[b], B. J. Merrill[b], D. A. Petti[b], H. Nishimura[c], M. Nishikawa[a], T. Terai[c], S. Tanaka[c]

a Department of Applied Quantum Physics and Nuclear Engineering, Kyushu University,
Hakozaki, Higashi-ku, Fukuoka 812-8581, Japan
b Idaho National Engineering and Environmental Laboratory (INEEL),
P. O. Box 1625, Idaho Falls, ID 83415, USA
c Department of Quantum Engineering and Systems Science, University of Tokyo,
Hongo, Bunkyo-ku, Tokyo 113-8656, Japan

Experiment of deuterium permeation through Ni facing with purified Flibe is being carried out under the Japan-US joint research project (JUPITER-II). The experiment has been proceeding in the following phases; (i) fabrication and assembly of a dual-probe permeation apparatus, (ii) a single-probe Ni/D_2 permeation experiment without Flibe, (iii) a dual-probe Ar/Ni/D_2 permeation experiment without Flibe, (iv) Flibe chemica purification by HF/H_2 gas bubbling, (v) physical purification by Flibe transport through a porous Ni filter, (vi) Ar/Ni/Flibe/Ni/D_2 permeation experiment using the dual Ni probe, and (vii) Ar/Ni/Flibe/Ni/HT permeation experiment. The present paper describes results until the Ar/Ni/Flibe/Ni/D_2 permeation experiment in detail.

1. INTRODUCTION

Flibe (2LiF + BeF_2 molten salt mixture) is a promising candidate for a liquid breeding material of a fusion reactor [1,2]. Many physical and chemical properties of Flibe were determined previously in the molten salt experimental reactor program of ORNL [3]. Although tritium permeating through structural materials from a Flibe blanket is a critical issue for the safety of a fusion reactor application, behavior of tritium permeation in Flibe and through Flibe-facing materials are less understood except for previous studies [1,4,5]. So, an experimental effort was initiated recently at INEEL as part of the Japan/US joint research project (JUPITER-II) [6] to investigate the behavior of hydrogen isotopes in Flibe and through Flibe-facing materials. Other JUPITER-II studies carried out at INEEL concern Flibe handling, mobilization, Redox control by Be and Flibe safety. In our initial studies [7,8], we designed a cylindrically-symmetric, dual-probe permeation device, conducted extensive TMAP4 analytical simulation to quantify tritium behavior in the Flibe/tritium pot experimental system, and experimentally evaluated Flibe containment materials suitable for Flibe/tritium behavior experiments. In the present study, we will show results of our recent experimental studies with a dual-probe permeation system, with an emphasis on deuterium experiments and accompanying analysis.

The deuterium/tritium permeation experiment using the dual-probe configuration in a pot containing molten Flibe is being down in several phases: (i) fabrication and assembly of the dual-probe experimental system; (ii) tests of the single probe system with deuterium, no Flibe, and mass-spectrometer gas analysis; (iii) tests of the dual-probe system with deuterium and without Flibe; (iv) chemical purification by HF/H_2 gas bubbling, (v) physical purification by transport through a porous Ni metal filter, (vi) experiments of the dual-probe system with deuterium, with Flibe, and mass-spectrometer gas analysis, and (vii) experiments of the dual-probe system with tritium, Flibe, and on-line tritium analysis. The experimental work is complemented by extensive model simulation using the TMAP4 computer code [9]. This paper summarizes the status to date of this effort. The overview of Flibe studies carried out in INEEL is presented by another paper in this Be workshop [10].

2. EXPERIMENTAL

2.1. Permeation Probe and Pot

Figures 1 and **2** show photos of the dual-probe permeation pot. **Figure 3** shows a schematic illustration of the experimental apparatus. It consists of a 316 stainless-steel pot, a nickel crucible for containing Flibe, two permeation probes of thin-walled nickel, a gas manifold, and associated pumps and sensors. The experiment vessel can contain about 800 g of Flibe that was purified by a HF/H_2 gas bubbling method at 550 to 600 °C to remove carbon, carbonates and oxide impurities. Hydrogen and argon and helium were purified by metal getters.

The probes/pot system was designed based on the following considerations: (i) one-dimensional permeation, (ii) easy manipulation, (iii) low tritium leak to the glove-box atmosphere, and (iv) low tritium inventory. The upper parts of the inner and outer probes were covered by respective barrier probes in order to eliminate effects of tritium (or deuterium) permeating through cover gas (Ar or He) over Flibe.

A smaller flange with 7 ports and a central Ni probe (probe 1) and a larger flange with 6 ports and an outer Ni probe (probe 2) were manufactured at INEEL as seen in overview photos of the pot and two probes of Figs. 1 and 2. Probe 1 was pressurized with deuterium/tritium. The D/T quantity permeating into Probe 2 was measured by on-line quadrupole mass spectrometer (QMS) or tritium-counting techniques. The Ni-probe components were fabricated from 0.5-mm Ni sheet using laser welding. Because of the complexity of the fabrication process, the components were tested at various stages of fabrication and assembly with a He leak detector to assure leak-tightness of the components. After confirming no leak

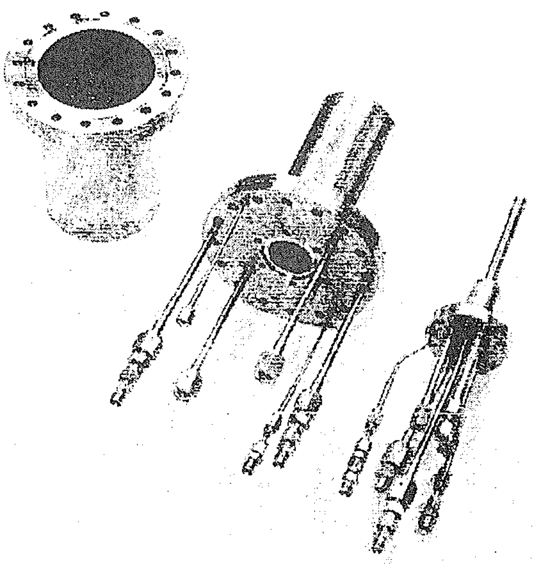

Fig. 1 Inner and outer probes and a pot

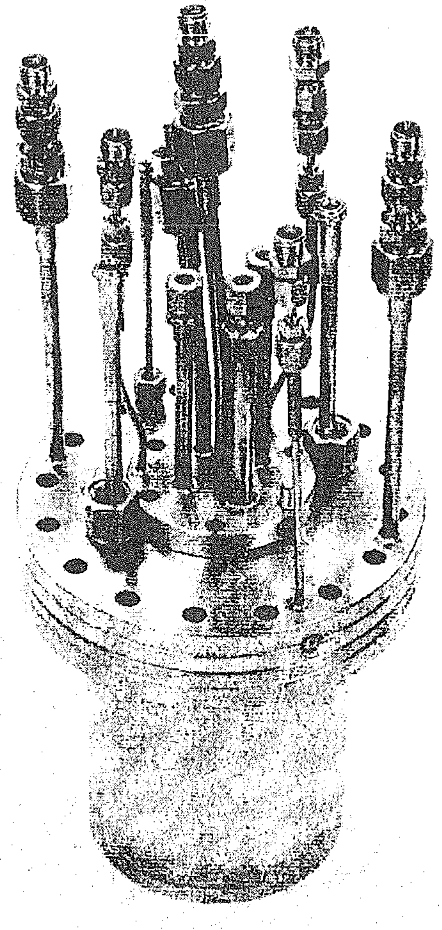

Fig. 2 Dual-probe Flibe/D_2 permeation pot

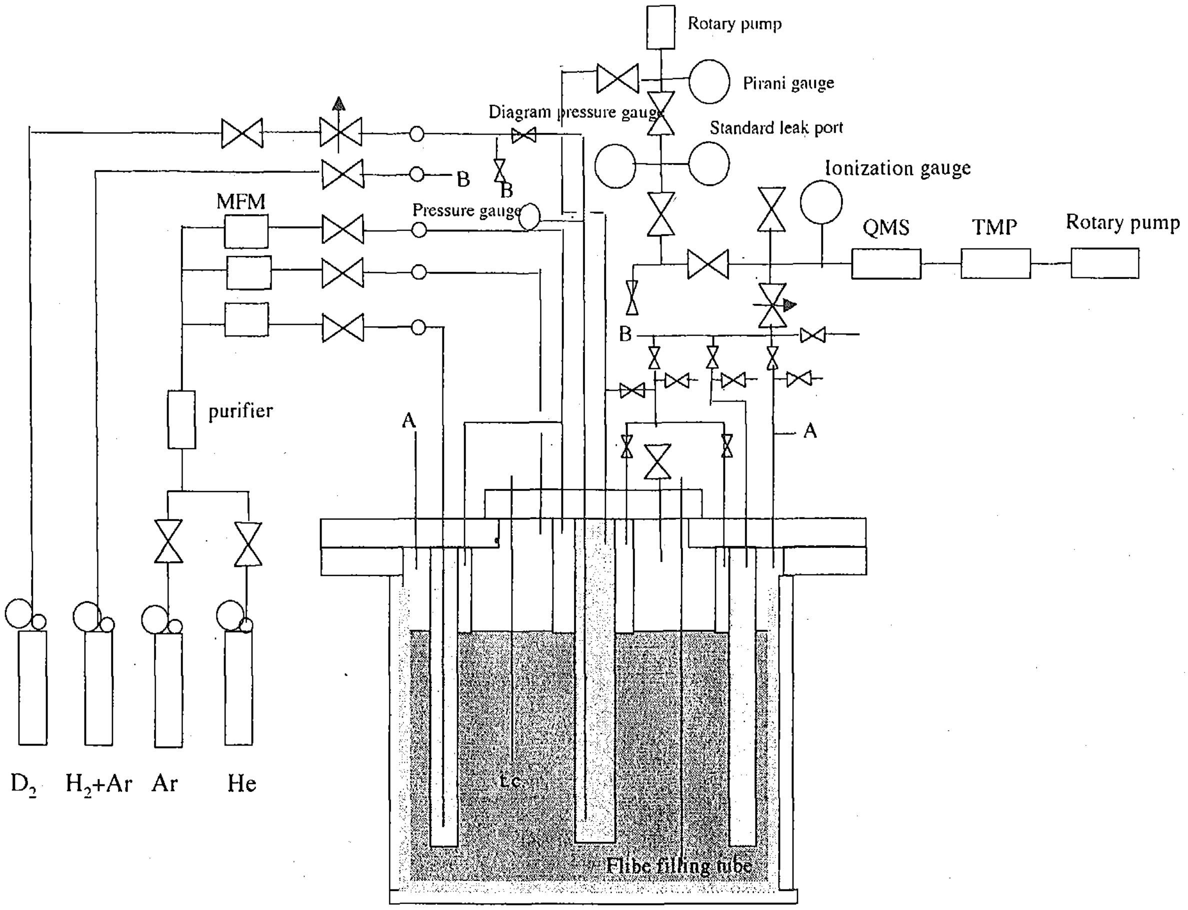

Fig. 3 A schematic illustration of Flibe/D_2 permeation apparatus

in the two probes, we set up the single-probe and dual-probe Ni-permeation apparatuses in the tritium-handling globe-box in the INEEL tritium laboratory [10,11]. All gas lines from the pot/probe assembly to the gas supply ports and to the gas analysis system were connected.

Baking of the Ni pot + probes up to 600 °C was carried out under evacuation by a turbo-molecular pump for one day. Thermal cycle tests were repeated. There was no gas release from the pot and probes during heating and evacuating. There was no background peak of m/e = 4. The base pressure of the QMS vessel was around 1×10^{-10} mmHg. That of the pot was a little greater than 1×10^{-6} mmHg. The pressure difference was due to the low conductance of a valve and line connecting the Ni pot with the QMS vacuum system. Therefore, we decided to carry out the D_2 permeation experiment by Ar gas purge in the pot with on-line analysis of the Ar purge gas with QMS and sampling valve arrangement. Four mass flow meters installed in gas supply lines were calibrated using a bubble-tube flow measurement device and provided an accuracy of about 2 %.

The QMS measurement of deuterium concentrations in the Ar purge gas was calibrated using three different standard concentrations of hydrogen gas in Ar balance, 100 ppm, 500 ppm and 5014 ppm. Linearity between the hydrogen concentration and the peak height ratio of m/e=2 to m/e=40 in QMS was made sure. A correction factor between the QMS peak height and the hydrogen or deuterium concentration was determined.

Table 1 Analytical Results from Purification (ppm)

	As-melted condition (top material)	**As-melted condition (salt sample)**	**Post H_2/HF treatment (salt sample)**
Batch No. 2			
Carbon	46,700	970	45
Oxygen	-------	(1140-2280)	607
Iron	-------	(90-260)	(165-176)
Nickel	-------	(20-60)	(85-87)
Chromium	-------	<25	(18-19)
Batch No. 3			
Carbon	-------	1700	-------
Oxygen	-------	(1040-1620)	-------
Iron	-------	(140-300)	-------
Nickel	-------	(45-65)	-------
Chromium	-------	<7	-------

Note: The metallic impurities and oxygen showed greater variability in the as-melted condition compared to better homogeneity after the H_2/HF treatment. White or clear pieces of salt showed lower levels of these impurities. Darker or spotted pieces had higher concentrations.

2.2. Flibe Purification

Flibe was manufactured by heating and melting a mixture of LiF and BeF_2 powders in a carbon crucible. The molar ratio was 2:1. Since the BeF_2 and LiF powder could adsorb water vapor, the powder mixture was heated up to 250 °C under He + 5%H_2 gas purging for one day in order to dry it before melting. The upper limit of temperature was decided in order to avoid LiOH generation. Flibe melting was performed with keeping the temperature at 600 °C for one day.

Chemical purification of Flibe was carried out using a HF/H_2 gas bubbling way based on a technique of the previous molten salt reactor program [3]. The inlet molar fraction ratio was HF/H_2=1/10. Hydrogen fluoride was supplied with a gas cylinder heated up to 40 °C to give around 2 atm HF vapor pressure. The all gas lines from the HF gas cylinder to the pot including a mass-flow controller and valves were made of a Ni alloy in order to avoid corrosion by HF. The amount of HF consumed for the chemical purification was determined by the titration of NaOH aqueous solutions. The HF/H_2 gas bubbling and titration measurement were continued for 6 days.

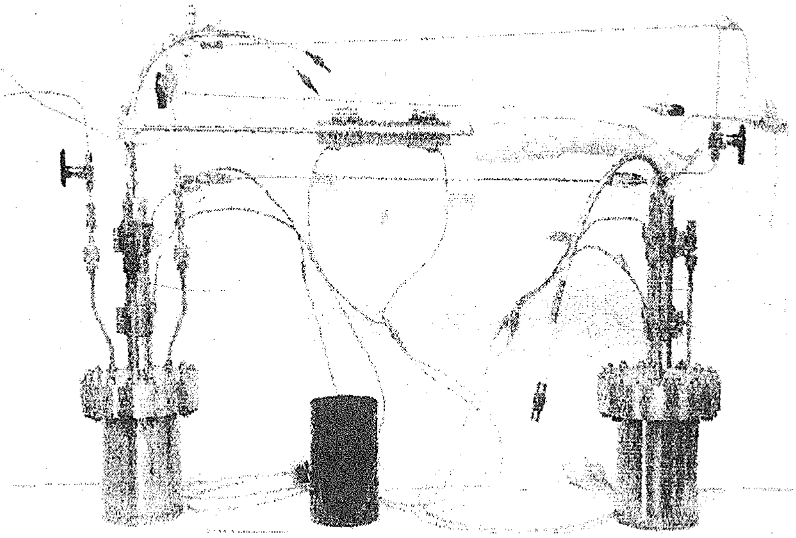

Fig. 4 Flibe transport and physical purification system

Contents of oxygen, nitrogen and carbon before and after purification were determined by an impurity analyzer of LECO, and other metal impurities were done by Inductively Coupled Plasma-Atomic Emission Spectrometer (ICP-AES). As seen in **Table 1**, oxygen and carbon concentrations in the as-melted Flibe were 2280 ppm and 970 ppm, respectively. Those after the HF/H_2 treatment for 6 days were 607 ppm and 45 ppm. Impurity gases including oxygen and carbon atoms were swept in molecular forms of H_2O, CO, CO_2, CH_4 and so on with the HF/H_2 gas supplied.

Figure 4 is a photo of an experimental apparatus for Flibe physical purification using a porous Ni filter and for Flibe transfer from the purification pot to the permeation pot that was set up in another Be-handling glove-box. The physical purification was carried out to remove a carbon impurity layer located at the top layer of Flibe. The 0.25-in. transfer line included the Ni filter, three detachable Cu covers and heaters over connector components, and additional heaters around the transfer tube to maintain good thermal uniformity. Each pot had two gas inlet/outlet ports, a thermocouple port and a transfer tube. A receiver pot had another port for a level sensor made of Ni. The three copper blocks could be detached from the transfer line in order to make it easy to bring up and down the connecting tube in a glove box. All tubing was designed to be compact in order to handle it easily in the globe-box. Transfer of Flibe between the two pots was successfully carried out. Physical purification, i.e. removal of impurity particles, could be achieved successfully.

3. RESULTS AND DISCUSSION

3.1. Single-Probe Ni/D_2 Permeation Experiment

The single-probe-permeation experiment was performed to check the central probe, the gas flow system through the pot and the detection system. These measurements were important to verify the permeation behavior of the Ni probe and pot for the Flibe studies. The experiment was performed under different conditions of Ar gas flow rates in the pot from 25 cm^3(NTP)/min to 500 cm^3(NTP)/min, and different temperature conditions of 833 K to 985 K under a constant Ar flow rate.

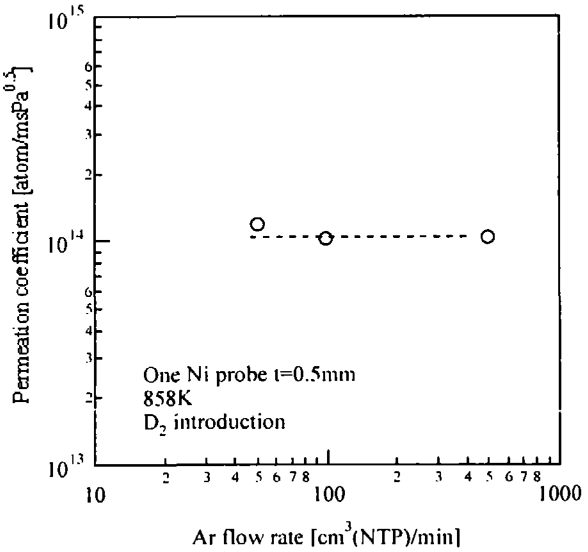

Fig. 5 Variations of Ni permeability with flow rate

All permeation experiments were carried out in the following procedure: (i) heating up the pot to a specified temperature under a constant Ar gas purge flow rate of the pot and probes, (ii) evacuation of the inner Ni probe by a roughing pump down to 0.03

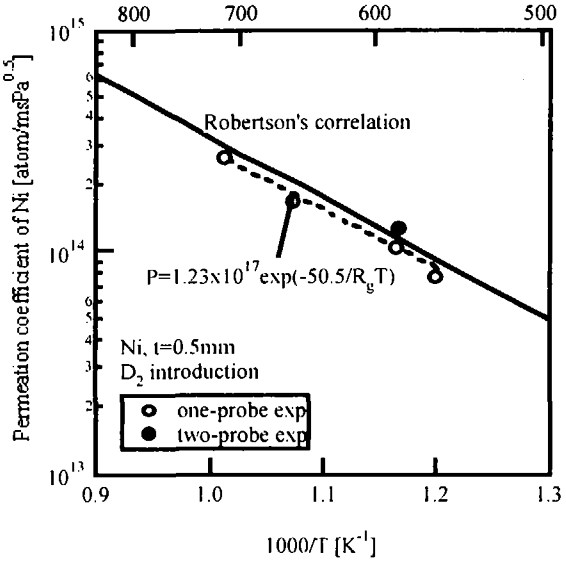

Fig. 6 Variations of Ni permeability with temperature

mmHg, (iii) D_2 gas introduction to the inner probe at 690 mmHg through a metering valve (this is the start of permeation "build-up run"), (iv) continuous monitoring of the pot temperature, the D_2 pressure in the probe, the residual gas spectrum in Ar purge gas by QMS and other experimental conditions, (v) after confirming a steady-state permeation rate, evacuating the probe and introducing Ar gas purge into the probe under the condition of 25 cm^3(NTP)/min (this is the start of permeation "decay run"), (vi) after sufficient time passing to follow the decay transients, terminating the gas analysis; (vii) cooling down the pot temperature to room temperature or moving to another experimental condition while Ar gas purge.

All data were correlated based on our numerical simulation using the TMAP4 code [9]. The calculations were in good agreement with experimental ones. The transient build-up data gave us information that mixing of deuterium in Ar is the rate-limiting process of the D_2 build up, and effect of H-diffusion in Ni is limited in about one minute after the initial transient permeation. The transient decay data showed that D-desorption from Ni surfaces is so fast that its rate is limited by the Ar flow rate in a similar way to the build-up run.

The permeation coefficient of D atom through Ni was determined from steady-state D_2 and HD concentrations in Ar purge gas in the pot. As shown in **Figs. 5** and **6**, the values of the permeability for various temperatures were coincident with the product of the equations of H-diffusivity and H-solubility in Ni that were given by W. E. Robertson [12,13], who correlated around 20 data previously. The steady-state permeability was independent of Ar flow rates as shown in Fig. 5. Consequently, the deuterium permeation was considered to be limited by diffusion through Ni. The effect of thermal transpiration [14] was found to be negligibly small, and the isotope effect between H and D permeation was found to be within previous reference data [15].

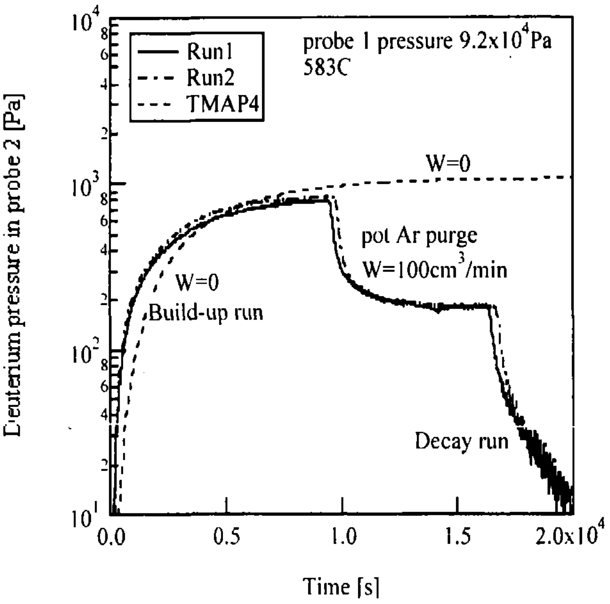

Fig. 7 Results of dual-probe Ni/D_2 permeation experiment

3.2. Dual-Probe Ni/D_2 Permeation Experiment

Since all permeation data of the present single-probe system were consistent with previous ones of H-permeation through Ni [13], we moved to the dual-probe system.

When we defined the deuterium sweep rate in the pot as j_{pot}, a relation in permeation rate between the probe 1, j_1, and probe 2, j_2, was expressed by Eq. (1):

$$j_2 = j_1 - j_{pot} \qquad (1)$$

The steady-state deuterium permeation flux, j_D, is given by Eq. (2) described below. Here, r_0, r_1, p_0 and p_1 are inner and outer diameters and pressure of the probe 1, and r_2, r_3, p_2 and p_3 are those of the probe 2. The height of the two probes is denoted by l, and D_{Ni}, D_{Flibe}, K_{Ni} and K_{Flibe} are diffusivity and solubility of Ni and Flibe.

Figure 7 is an example of the D_2 permeation rate using the two probes without Flibe. The build-up curves of the two runs were compared with the

$$2\pi r l j_D = -\frac{2\pi l D_{Ni} K_{Ni}\left(\sqrt{p_0}-\sqrt{p_1}\right)}{\ln\left(\frac{r_0}{r_1}\right)} = -\frac{4\pi l D_{Flibe} K_{Flibe}\left(p_1-p_2\right)}{\ln\left(\frac{r_1}{r_2}\right)} = -\frac{2\pi l D_{Ni} K_{Ni}\left(\sqrt{p_2}-\sqrt{p_3}\right)}{\ln\left(\frac{r_2}{r_3}\right)} \qquad (2)$$

simulation using the TMAP4 code. Reproducibility of the D_2 permeation rates was good, and the transient build-up curves were also in good agreement with the simulation curve. The permeability of the two probes were in good agreement with that of the single-probe experiment as well as previous permeability data [12]. Thus, these results demonstrated the suitability of our mass-spectrometric approaches for measuring downstream permeation rates.

At around 9000 sec after the start of D_2 permeation, we began an argon purge with 100 cm^3(NTP)/min through the pot. Then, the deuterium concentration in the probe 2 started decreasing quickly and approached another deuterium concentration.

3.3. Rate-Determining Step of Flibe/Ni/D_2 System

When molten Flibe is stagnant in the pot, we calculated overall deuterium permeation rates in the Flibe/Ni/D_2 system by the TMAP4 code. **Figure 8** shows the rate-determining step for the D_2 permeation from Flibe through Ni to Ar gas purge. It was found that diffusion in Flibe is the rate-determining step under common pressure conditions. Migration through impurity layer formed on Ni can be the rate-determining step only when the surfaces are contaminated heavily. This is because the overall permeation rate decreased strongly around one thousandth of the case without Flibe. The diffusion coefficient through Flibe was much smaller than Ni one. When Flibe is flowing under hydrogen pressure higher than 10^{10} Pa, the rate-determining step was considered diffusion through a Ni tube.

When the rate-determining step is diffusion in Flibe in the dual-probe system, the governing equation of deuterium permeation could be integrated analytically both in the rectangular coordinate and in the cylindrical coordinate. The solution of permeation flux j for the cylindrical coordinate is expressed by Eq. (3):

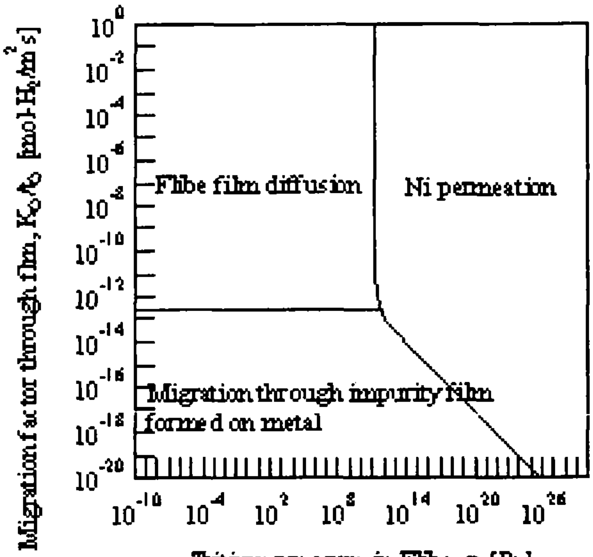

Fig. 8 Rate-determining step of Flibe/Ni/D_2 system

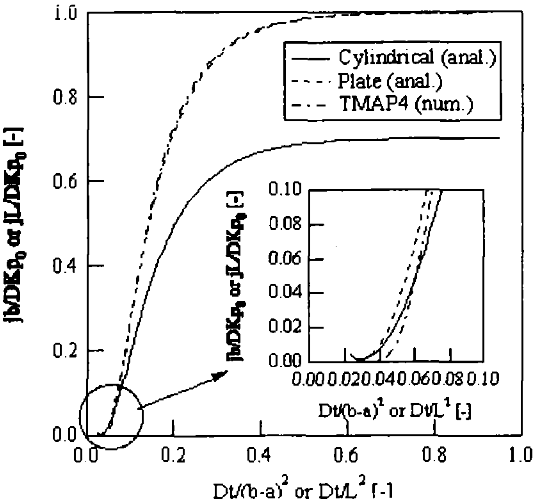

Fig. 9 Comparison between TMAP4 and analytical solution

Here, a and b are radii of the inner probe and outer probe, and J_0 and N_0 are the zeroth-order, the first-kind and second-kind Bessel functions. The values of α_n were determined as roots of Eq. (4).

$$\frac{jb}{DKp_0} = \frac{1}{\ln\left(b/a\right)} - \sum_{n=1}^{\infty} \frac{2J_0(a\alpha_n)J_0(b\alpha_n)\exp\left(-\alpha_n^2 Dt\right)}{\left(J_0(b\alpha_n) - J_0(a\alpha_n)\right)\left(J_0(b\alpha_n) + J_0(a\alpha_n)\right)} \qquad (3)$$

$$N_0(a\alpha_n)J_0(b\alpha_n) = N_0(b\alpha_n)J_0(a\alpha_n) \qquad (4)$$

Figure 9 shows an example of the comparison between the TMAP4 calculation and the analytical solution. The two of the dotted line and the chain line in the figure show the TMAP4 calculation and the analytical solution for the rectangular coordinate, respectively. They agreed well in the whole region. In a similar way, the two of the chain line and the solid line also agreed well in the narrow region where breakthrough in the deuterium concentration started. However, the steady-state deuterium flux was different between the two lines. This was because the TMAP4 is based on the rectangular coordinate, while the analytical solution is based on the cylindrical coordinate. In the present dual-probe system, experimental data of the deuterium permeation flux were correlated by the analytical solutions of Eq. (3) and (4).

The results of the rate-determining step calculation meant also that tritium diffusivity in Flibe is the most important factor for designing systems for the recovery of tritium from flowing or stagnant Flibe blankets, such as a Flibe-He counter-current flowing column and a tritium permeation window [16,17].

3.4. Dual-Probe Ar/Ni/Flibe/Ni/D$_2$ Permeation Experiment

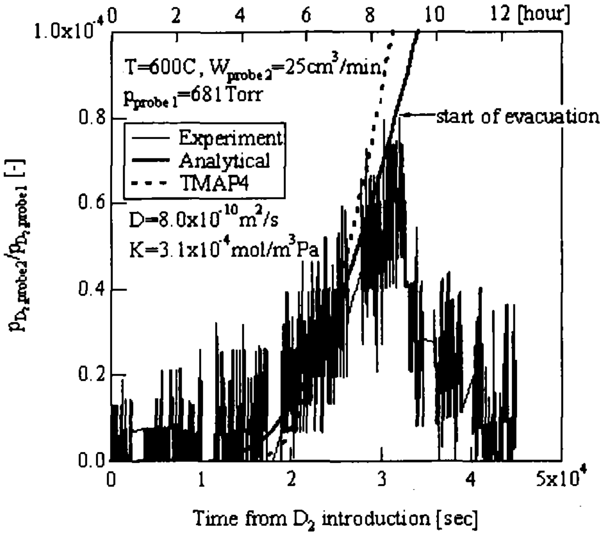

Fig. 10 Results of dual-probe Flibe/Ni/D$_2$ permeation

Flibe purified chemically and physically was transferred to the dual probe Ni pot in the globe box. **Figure 10** shows an example of the experimental results of deuterium permeation through the Ar/Ni/Flibe/Ni/D$_2$ system. Since the deuterium partial pressure in Ar sweep gas was near to the background level of the QMS, some noises appeared in the output spectrum. Nevertheless, close agreement was obtained between the experiment and the analytical solution. Fitting two curves gave a set of diffusivity and solubility of deuterium in Flibe, defined by D_D and K_D, respectively.

Figures 11 and **12** show values of the diffusivity and solubility of deuterium in Flibe determined from the curve fitting. Experimental temperature was 600 °C and 650 °C.

Previously, two correlations on diffusivity of hydrogen isotopes were reported for solid Flibe below its melting point (chain line) [18] and for molten Flibe

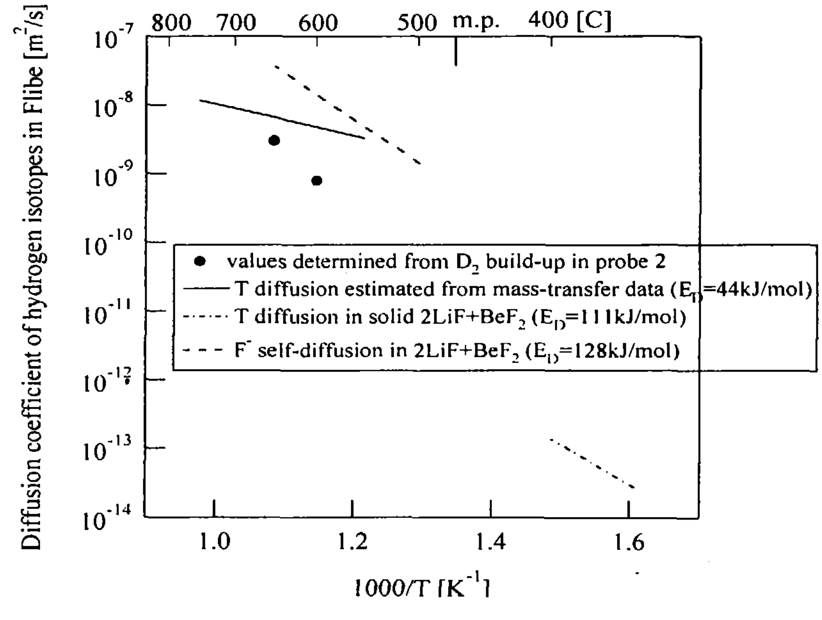

Fig. 11 Diffusion coefficient of D in Flibe

above it (solid line) [19]. The latter investigated the behavior of tritium diffusion in molten Flibe irradiated by neutron in terms of a mass-transfer coefficient, and diffusivity of the hydrogen isotope was calculated by R. Anderl [20]. The values of the diffusivity of D in molten Flibe determined in the present nonirradiated study (painted circles) ranged from 8×10^{-10} m²/s at 600 °C to 3×10^{-9} m²/s at 650 °C.

The activation energy of the viscosity and the electrical conductivity of Flibe was 38 kJ/mol [21]. On the other hand, F^- ion self-diffusivity in molten Flibe was 128 kJ/mol that was determined using F^{18} isotope [22]. Thus, there was much difference in the two activation energies, judging from the Stokes-Einstein equation. This might be because chemical conditions of Flibe molten salt for previous experiments were different. These values of tritium diffusivity of previous molten Flibe [19,20] were not too different from what we determined. However, the activation energy was quite different.

The previous ORNL study showed that the viscosity of mixtures of LiF + BeF_2 decreased rapidly with an increase of the LiF concentration [21], due to breaking of the fluorine bridges in a three-dimensional network of Be-F bonds. In the 2LiF + BeF_2 molten mixture, all network of the Be-F bonds was considered to disappear. The tetrahedral BeF_4^{2-} ion should be predominant in the molten 2LiF + BeF_2 mixture. Since the Be-F bonds almost disappeared, the activation energy of Flibe viscosity was comparatively small. However, if a small amount of free fluorine ions were left in molten Flibe, deuterium ion dissolved in Flibe would combine with the free fluorine ion. In that case the diffusion mechanism should be different between Flibe viscosity and hydrogen isotope diffusivity. The activation energy of the deuterium diffusivity determined in the present study was close to the F^- ion self-diffusivity. This is reasonable to expect that the F^- ion self-diffusivity and deuterium diffusivity had a similar activation energy, because two atoms of D and F diffused in molten Flibe in a similar way.

There were one correlation available on solubility of D_2 in Flibe previously [23]. The data were compared with the present solubility data as seen in Fig. 12. The solubility determined in the present study was about thousands time larger than the previous D_2 solubility data. This is because the chemical potential of deuterium in Flibe was higher than the expected chemical potential of D solute when the dominant species of deuterium in Flibe was D_2. The value of deuterium solubility determined by the permeation data was much nearer to the DF solubility determined

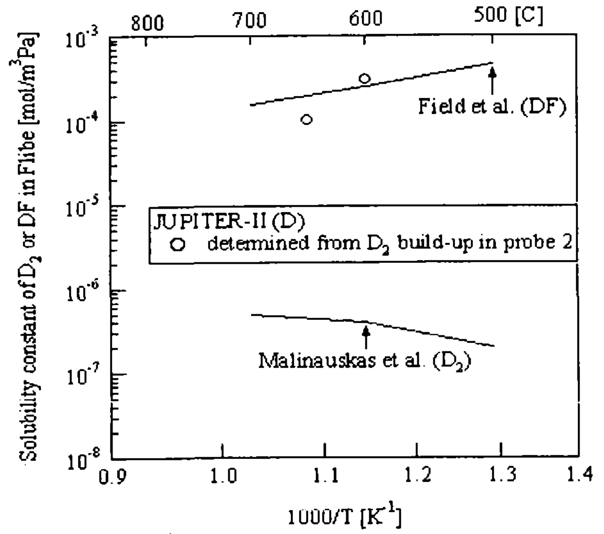

Fig. 12 Solubility constant of D_2 and DF in Flibe

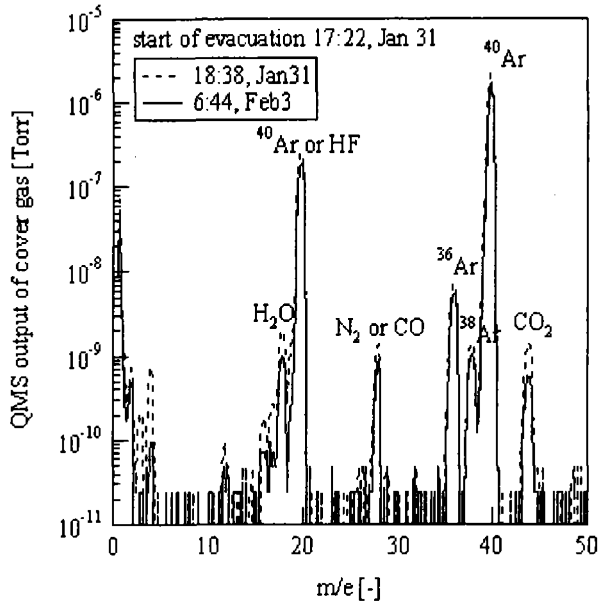

Fig. 13 Mass spectrum of Ar cover gas over Flibe

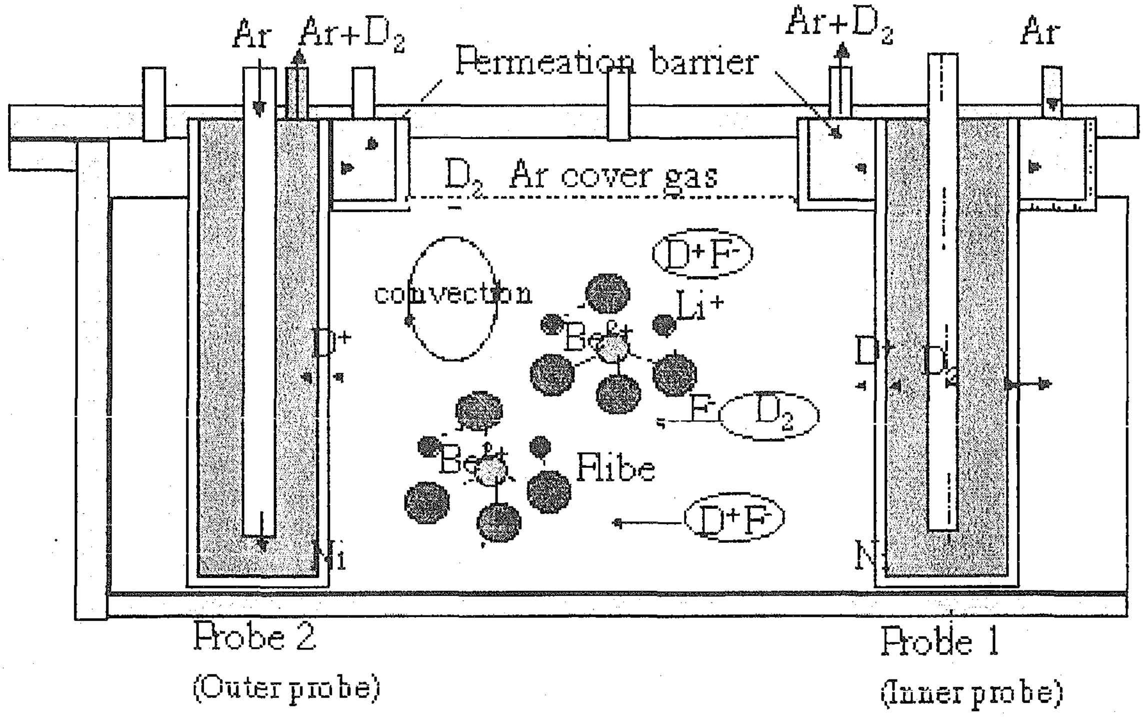

Fig. 14 Schematic illustration of deuterium diffusion in Flibe of Ar cover gas over Flibe

previously [24]. This seemed to be because the dominant species of deuterium in Flibe was DF.

After the second run of Jan 31, the two inner and outer probes were evacuated by a associated turbo-molecular pump, while Ar purge in Flibe cover gas was continued. **Figure 13** shows variations of the QMS spectrum of Ar cover gas with time after the permeation experiment. As seen in the figure, the QMS spectrum of several impurity peaks corresponding to m/e=18, 28, 44 and so on decreased during the four-days Ar gas purge. Therefore, we could guess that a small amount of HF remaining in Flibe after the HF/H_2 chemical purification still reacted with several impurities. This was the reason for that the predominant species of deuterium in Flibe was DF. Complete desorption of HF from molten Flibe was difficult by He gas bubbling. Be Redox control seemed to be a promising way to convert HF to H_2 in Flibe.

3.5. Discussion of Hydrogen Isotope Behavior in Flibe

Figure 14 shows a schematic illustration of the dual-probe Flibe pot system. Deuterium atoms dissolved in Flibe through the inner probe wall. Almost all ions in the Flibe molten salt comprised the tetrahedral structure of BeF_4^{2-} ions and Li^+ ions. Dissolved deuterium atoms combined with free fluorine left in Flibe purified by the HF/H_2 gas bubbling. Consequently, the dominant species of deuterium was DF. The DF molecules diffused in bulk Flibe. When the DF arrived at the outer probe, the DF molecules dissociated to D^+ and F^- ions on Ni surfaces. Only D atoms permeated through Ni walls and was swept by Ar gas.

As seen in **Figure 15**, temperature difference of around 30 °C was present in the Flibe pot. Therefore, a small convection was seemed to occur in the pot. The convection should affect the performance in deuterium diffusion in bulk Flibe. At present, another numerical calculation is being carried out in order to make clear the effects of thermal convection on deuterium diffusion in Flibe. Further, another pot design was also under way in order to eliminate the thermal convection as low as possible.

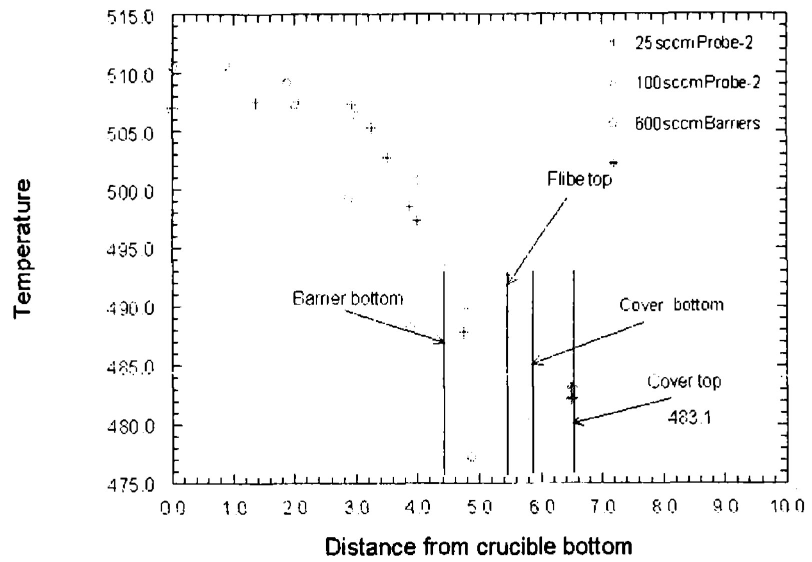

Fig. 15 Temperature profiles in Flibe/D_2 pot

4. CONCLUSIONS

Under the research project of JUPITER-II, we performed the experiments of Ni/D_2 permeation through the single and dual probes and Ni/Flibe/D_2 permeation using purified Flibe. Regardless of single or dual probes, D_2 permeation rate through Ni was in good agreement with previous works. The present dual-probe permeation system was found to work well in terms of the Ni permeability, gas flow system through the pot and probes and the detection system. It was expected that the present probe/pot system can provide a suitable device to determine the solubility and diffusivity of tritium in Flibe and tritium permeability through Ni facing Flibe.

On Flibe purification, we carried out chemical purification by HF/H_2 gas bubbling and physical purification by Flibe transport through a porous Ni filter. Most of carbon and oxygen impurities in as-melted Flibe were removed by the chemical purification and the physical purification.

Diffusivity and solubility of deuterium in Flibe were determined using the dual-probe Ni pot system. The dominant species of deuterium was DF judging from diffusivity and solubility data. The diffusivity of deuterium ranged from 8×10^{-10} m^2/s to 3×10^{-9} m^2/s at 600 - 650 °C. The solubility of deuterium was near to the DF solubility data obtained previously. Redox control experiment using Be is being carried out. Preliminary experiment showed that the HF concentration heavily decreased by dipping Be in Flibe. After the Redox control experiment, we will continue tritium permeation experiment using Redox-controlled Flibe.

REFERENCES

[1] D. -K. Sze, M. Sawan and E. T. Cheng, "Impact of Transmutation in Fusion Environment on Flibe Chemistry", Fusion Technol., 39 (2001) 789-792.

[2] A. Sagara, H. Yamanishi, T. Uda, O. Motojima, T. Kunugi, Y. Matsumoto, Y. Wu, H. Matsui, S. Takahashi, T. Yamamoto, S. Toda, O. Mitarai, S. Satake, T. Terai, S. Tanaka, S. Fukada, M. Nishikawa, A. Shimizu and N. Yoshida, "Studies on Flibe Blanket Designs in Helical Reactor FFHR", Fusion Technol., 39 (2001) 753-757.

[3] J. H. Shaffer, "Preparation and Handling of Salt Mixtures for the Molten reactor Experiment", ORNL-4616, (1971).

[4] H. Moriyama, S. Maeda, T. Ohmura, K. Moritani and J. Oishi, "Chemical Behaviors of Tritium Formed in a LiF-BeF_2 Mixture", J. Nucl. Mater., 148 (1987) 211-216.

[5] H. Nishimura, A. Suzuki, T. Terai, M. Yamawaki, S. Tanaka, A. Sagara and O. Motojima, "Chemical Behavior of Li_2BeF_4 Molten Salt As a Liquid Tritium Breeder", Fus. Eng. Des., 58-59 (2001) 667-672.

[6] D. A. Petti, R. A. Anderl, D. -K. Sze, T. Terai and S. Tanaka, "Jupiter-II Flibe Tritium/Chemistry and

Safety Experimental Program", Fusion Sci. Technol., 41 (2002) 807-811.

[7] S. Fukada, R. A. Anderl, Y. Hatano, S. T. Schuetz, R. J. Pawelko, D. A. Petti, G. R. Smolik, T. Terai, M. Nishikawa, S. Tanaka and A. Sagara, "Initial Studies of Tritium Behavior in Flibe and Flibe-Facing Material", Fus. Eng. Des., 61-62 (2002) 783-788.

[8] S. Fukada, R. A. Anderl, R. J. Pawelko, G. R. Smolik, S. T. Schuetz, J. E. O'Brien, H. Nishimura, Y. Hatano, T .Terai, D. A. Petti, D. K. Sze, S. Tanaka, "Flibe-D_2 Permeation Experiment and Analysis", Fus. Sci. Technol., Vol. 44, No. 2 (2003) 415-419.

[9] G. R. Longhurst, D. F. Holland, J. L. Jones and B. J. Merrill, "TMAP4 User's Manual", EGG-FSP-10315, (1998).

[10] R. A. Anderl, D. A. Petti, G. R. Smolik, R. J. Pawelko, S. T. Schuetz, J. P. Sharpe, B. J. Merrill, M. F. Simpson, T. Terai, S. Tanaka, H. Nishimura, Y. Oya, S. Fukada, M. Nishikawa, K. Okuno, Y. Morimoto, Y. Hatano, D. -K. Sze, "Flibe molten salt research for tritium breeder applications", Proc. of BeWS-6, in printing.

[11] R. A. Anderl, D. A. Petti, K. A. McCarthy and G. R. Longhurst, "The Safety and Tritium Applied Research Facility", Fusion Sci. Technol., 41 (2002) 568-572.

[12] W. E. Robertson, "Hydrogen Permeation Diffusion and Solution in Nickel", Z. Metallkunde, 64 (1973) 436-443.

[13] F. Reiter, K. S. Forcey, and G. Gervasini, "Compilation of Tritium-Material Interaction Parameters in Fusion reactor Materials", EUR-15217-EN (1993).

[14] T. Takaishi and Y. Sensui, "Thermal Transpiration Effect of Hydrogen, Rare Gases and Methane", 2503-2514.

[15] S. Fukada, "Hydrogen Isotope Separation by Hydrogen-Absorbing-Alloy Beds", Tokyo, NTS, (2000) ISBN4-900830-55-0.

[16] S. Fukada, M. Nishikawa and A. Sagara, "Calculation of Recovery Rates of Tritium from Flibe Blanket", Fusion Technol., 39 (2001) 1073-1077.

[17] S. Fukada, M. Nishikawa, A. Sagara and T. Terai, "Mass-Transport Properties to Estimate Rates of Tritium Recovery from Flibe Blanket", Fusion Sci. Technol., 41 (2002) 1054-1058.

[18] H. Moriyama, J. Oishi and K. Kawamura, "The effects of fusion neutron irradiation on tritium recovery from lithium salts", J. Nucl. Mater., 161 (1989) 197-203.

[19] J. Oishi, H. Moriyama, S. Maeda, Y. Asaoka, "Tritium recovery from molten LiF-BeF_2 salt", Fus. Eng. Des., 8 (1989) 317-321.

[20] D. A. Petti, G. R. Smolik, R. A. Anderl, D. -K. Sze, S. Tanaka, T. Terai, A program plan for molten salt experiments being performed as part of the 2nd Japan/US program on irradiation tests for Fusion Energy Research (JUPITER-II) collaboration", INEEL/EXT-01-00796.

[21] S. Cantor, W. T. Ward and C. T. Moynihan, "Viscosity and density in molten BeF_2-LiF solutions", J. Chem. Phys., 50 (1969) 2874-2879.

[22] T. Ohmichi, H. Ohno and K. Furukawa, "Self-diffusion of fluorine in molten dilithium tetrafluoroberyllate", J. Phys. Chem., 80 (1976) 1628-1631.

[23] A. P. Malinauskas, D. M. Richardson, "The solubilities of hydrogen, deuterium and helium in molten Li_2BeF_4", Ind. Eng. Chem. Fundam., 13 (1974) 242-245.

[24] P. E. Field, J. H. Shaffer, "The solubilities of hydrogen fluoride and deuterium fluoride in molten salt fluorides", J. Phys. Chem., 71 (1967) 3218-3222.